12B.3 The variability of the ice crystal mass-size relationship in trailing stratiform precipitation systems using airborne Doppler cloud radar and in-situ microphysical observations

A. Protat *[1], J. Peter [1], E. Fontaine [2], A. Schwarzenboeck [2], and J. Delanoë [3]

[1] Centre for Australian Weather and Climate Research (CAWCR), Melbourne, Australia
[2] Laboratoire de Meteorologie Physique (LAMP), Clermont-Ferrand, France
[3] Laboratoire ATmosphere Mesures et Observations Spatiales (LATMOS), Guyancourt, France

1 INTRODUCTION

Cloud radars allow for the characterization of the vertical distribution of ice cloud microphysical properties through measurements of "moments" of the ice particle size distribution (the n^{th} moment of the particle size distribution N(D) is defined as

$$M_n = \int N(D)\, D^n \, dD . \qquad (1)$$

The cloud radar measured moments are the radar reflectivity (proportional to M_6 in Rayleigh approximation), and the terminal fall speed that can be retrieved from the Doppler radar measurement at vertical incidence or from a combination of non-collinear Doppler measurements (proportional to M_b where b varies with particle habit. Retrieving the microphysical properties from cloud radar measurements consists of retrieving for each radar range bin the two free parameters of a prescribed N(D) (two measurements for two unknowns) with two measured moments of N(D), and then to calculate the microphysical properties as proportional to moments M_0 for total concentration N_T, M_2 for visible extinction, M_3 for IWC, or M_3/M_2 for effective radius.

However additional assumptions about the statistical relationships between crystal mass and maximum crystal dimension $m(D_{max})$ and between projected surface and maximum dimension $A(D_{max})$ are needed in these calculations. In virtually all active remote sensing retrieval techniques, a single set of relationships is assumed for all ice clouds, with the exception of the RadOn technique (Delanoë et al. 2007), where this relationship is constrained by radar reflectivity and fall speed for each ice cloud. Generally, the Brown and Francis (1995) $m(D_{max})$ relationship for ice aggregates has been assumed in the past. Recent work has shown that this relationship provided accurate ice water contents (IWC) in a mean sense, but fails to capture dependences on temperature and particle size that are a result of the complex ice microphysical processes (Heymsfield et al. 2010, H10 in what follows). New $m(D_{max})$ relationships have therefore been proposed (H10) derived from closure analyses between particle size distribution and bulk IWC measurements in a variety of ice clouds from six field campaigns. However the variability of this relationship as a function of the large-scale conditions has also clearly been highlighted.

A large part of the errors in cloud microphysical retrievals is directly related to this natural variability when assuming a single $m(D_{max})$ relationship for all ice clouds, as recently highlighted for tropical cirrus clouds in Protat et al. (2011). Better constraints on the variability of the $m(D_{max})$ relationship are therefore needed to reduce uncertainties in ice clouds microphysical retrieval techniques using active remote sensing as input. The objective of this paper is to estimate the $m(D_{max})$ relationship using different types of closure analyses using collocated airborne cloud radar and in-situ microphysical measurements, and then to investigate the natural variability of this relationship. In section 2 we describe the observations used in this work. In section 3 we discuss the different closure analyses developed. We then analyse results obtained using these closure analyses in section 4.

2 OBSERVATIONS

In this work two main sources of observations are used: unique multi-beam airborne Doppler cloud radar observations and state-of-the-art in-situ N(D) and A(D) measurements. Such data have been collected in 2010 within the trailing stratiform part of continental Mesoscale Convective Systems (MCSs) over West-Africa (MT-2010). MT stands for Megha-Tropiques, a French-Indian satellite recently launched to investigate processes involved in the life cycle of MCSs, and the water and energy cycles in the Tropics.

2.1 The RASTA Airborne Doppler Cloud Radar

The RASTA (RAdar SysTem Airborne, Protat et al. 2009) radar is a 95.04 GHz multi-beam Doppler cloud radar installed on the French Falcon 20 research aircraft. During the MT-2010 experiment the integration in the aircraft included three downward-looking antennas (nadir, 38° off-nadir in the direction

* *Corresponding author address:* Alain Protat, CAWCR details; email: email @email

of propagation of the aircraft, and 20° off-nadir perpendicular to the direction of propagation of the aircraft.) and two upward-looking antennas (zenith, 38° off-nadir in the direction of propagation of the aircraft). So above the aircraft only two components of the 3D wind field can be retrieved. The RASTA radar has then been upgraded in 2011 to accommodate a third antenna looking up. We use the pulse pair signal processing, with 2048 pulses. The range resolution is 60m. The calibration of RASTA has been done using the ocean surface backscattering (the so-called "σ_0 method"). The sensitivity resulting from the different radar parameters was about -35 dBZ @ 1 km for the nadir antenna.

2.2 The in-situ microphysical probes

During MT-2010, the N(D_{max}) measurements of the in-situ microphysical properties were performed using a newer generation of Optical Array Probes (OAP): the 2D Stereo probe (2D-S) from SPEC Inc. and the Precipitation Imaging Probe (PIP) from Droplet Measurement Technologies. In order to derive particle size distributions, area distributions, and aspect ratios from the 2D images, standard corrections of the OAP data have been applied, including the rejection of 2D images where shattering or splash was identified. Moreover, truncated images which are partially recorded have been reconstructed and the pixel resolution has been corrected for the true air speed. Composite N(D_{max}) and A(D_{max}) distributions spanning 50 to 6400 microns in D_{max} have then been derived using a simple linear interpolation scheme described in Fontaine et al. (2013).

3 METHODOLOGY: CLOSURE ANALYSIS

There are different ways to extract information about the m(D_{max}) relationship from in-situ measurements. The first approach, used in H10, uses the in-situ N(D) and bulk IWC measurements to directly retrieve the a and b coefficients of the m(D_{max}) relationship expressed as m(D_{max}) = am (D_{max}) ^{bm}. This is expected to be the most accurate, since IWC is the integral of N(D_{max}) m(D_{max}) dD_{max}. However accurate bulk IWC measurements are not available during our field experiments. A second technique recently proposed in the literature (Protat et al. 2011) consists in using m(D_{max}) relationships from the literature weighted using the ice particle habit classification from the Cloud Particle Imager (CPI). It has been shown that the technique allowed for accurate retrievals of IWC in tropical cirrus, but it has not been tested in other types of ice clouds. Unfortunately the CPI was not part of the line-up either for MT-2010.

Two approaches using cloud radar and in-situ measurements are explored in this paper. The first approach (called METHOD1 below) is described in detail in Fontaine et al. (2013). The exponent bm of the m(D_{max}) relationship is first constrained by the exponent of the A(D) relationship, then the prefactor am of the m(D_{max}) relationship is constrained by the airborne cloud radar reflectivity interpolated at the flight altitude from the nadir and zenith radar beams. The tight relationship between the two exponents has been demonstrated using simulations of different particle habits (Fig. 1). The second approach (called METHOD2 below) has been discussed in the framework of the RadOn cloud radar retrieval technique (Delanoë et al. 2007). It consists in using radar reflectivity and terminal fall velocity retrieved from the airborne cloud radar data as references. The measured in-situ N(Dmax) and A(Dmax) are then used to generate a set of possible in-situ radar reflectivity (using T-matrix calculations with an aspect ratio of 0.6) and terminal fall velocity (using the Heymsfield and Westbrook 2010 parameterization). In order to generate this set of possible solutions we defined minimum and maximum values for the am and bm coefficients from the values published in H10 (Fig. 2). The retrieved optimal (am, bm) is the combination that provides smallest differences with radar reflectivity and fall speed in the least squares sense.

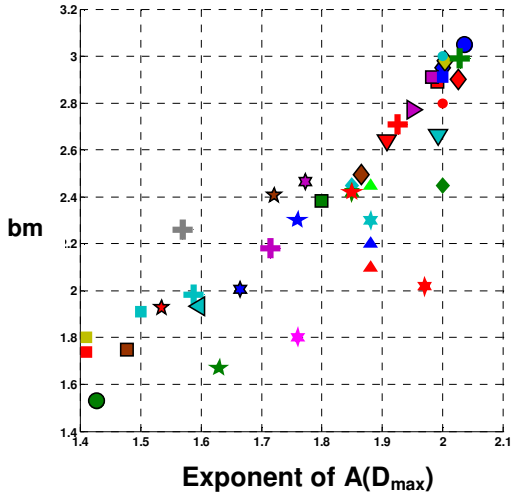

Figure 1: Relationship between the exponent of A(Dmax) and bm for several simulations of ice crystal habits.

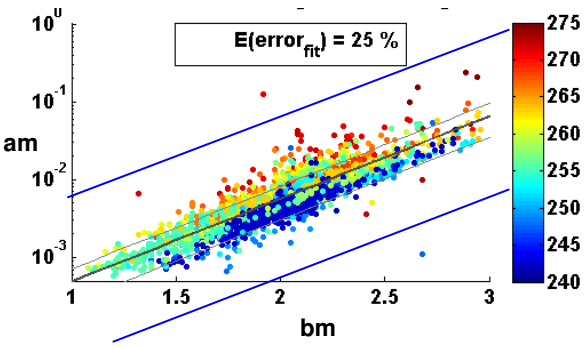

Figure 2: Relationship between am and bm and temperature dependence as derived from METHOD1 (see text). (a,b) boundaries for calculations of in-situ reflectivity and terminal fall speed in METHOD2 are also shown (blue lines).

4 RESULTS

4.1 Mass-size relationships with METHOD1

As discussed previously METHOD1 relies on a relationship between the exponent of the $m(D_{max})$ relationship and the exponent of the $A(D_{max})$ relationship. Each $N(D_{max})$ and the corresponding $A(D_{max})$ relationship has been derived from all in-situ microphysical observations from MT-2010 after averaging at 5 seconds resolution (which typically corresponds to a 1-km horizontal resolution at typical 200 ms^{-1} Falcon 20 aircraft speed). The RASTA radar reflectivities have also been averaged at 5 seconds resolution to match the in-situ measurements.

Figure 3 shows a summary of the variability of the am and bm coefficients of the $m(D_{max})$ relationship obtained from the MT-2010 flights.

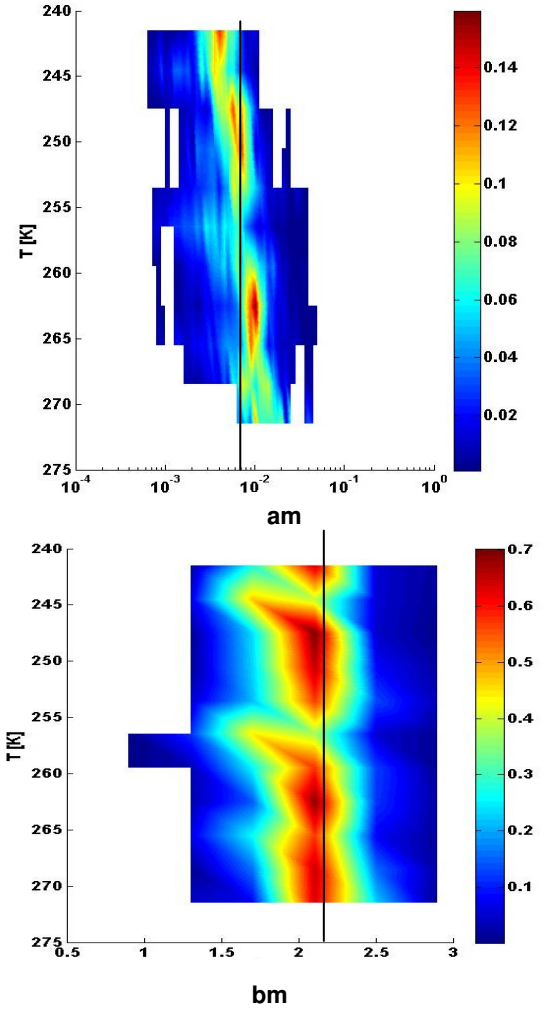

Figure 3: The probability distribution of a and b coefficients of the $m(D_{max})$ relationship as a function of temperature. The values of a and b from the H10 study are the black lines.

As can be seen from this figure the variability of the bm coefficient (lower panel) is smaller than that of the am coefficient. The standard deviation of the probability distribution of bm is quite small with 90% or more of points ranging between 1.6 and 2.4. The highest frequency values of the distribution are found for bm = 2.1 (60-70% at all heights) and does not vary with temperature. This small variaibility could be partly due to the fact that in METHOD1 the bm coefficient is linked through a parameterization with the exponent of the $A(D_{max})$ relationship, which might remove some of the natural variability. Such assumption is not made in METHOD2, so we will get back to this point below.

In contrast there is a clear tendency in Fig. 3 for the am coefficient to decrease with decreasing temperature (or increasing height in the troposphere). This temperature dependency is also shown in Fig.2, where the relationship between am and bm is given. This important result means that an ice particle of maximum diameter D_{max} will carry much less ice mass if located at greater heights in the troposphere. This is intuitively consistent with the fact that irregularly-shaped crystals are predominantly found at higher altitudes while more spherical ice aggregates are found at lower heights due to the aggregation process. The distribution of the am coefficient is also much wider than that of the bm coefficient with highest frequency values peaking at about 12-15% at all temperatures. This relatively large variability implies that the use of a single value of am for all clouds in ice cloud microphysical retrieval techniques is probably a major source of uncertainty. This will be quantified further in a follow-up study by running some sensitivity tests in a variational retrieval framework.

These results are very similar to those derived from the statistical study of H10 who used a very large number of field experiments and a variety of large-scale environments to propose:

$$m(D_{max}) = 5.28 \times 10^{-3} D_{max}^{2.1} \quad (2)$$

In their study, H10 also indicate that the variability of the am coefficient is a function of the large-scale regime the clouds are embedded in (convectively-generated versus synoptically-generated clouds). However they did not study the temperature dependence of the am coefficient. The value found in H10 in the immediate vicinity of deep convection (am=0.0110) is consistent with the values retrieved at temperatures from 273K down to about 260K in our West-African stratiform precipitation. Values similar to the composite value of H10 (am=0.00528) are found in our case higher up, or for temperature lower than 260K. If there is no way to further constrain the am coefficient in ice cloud microphysical retrieval techniques using active remote sensing observations, this vertical variability of the a coefficient could at least be introduced, and the width of the distribution could also be introduced in variational techniques within the error covariance matrix.

4.2 Mass-size relationships with METHOD2

As discussed previously METHOD2 uses two radar parameters instead of only the radar reflectivity in METHOD1. The terminal fall speed is retrieved from the system of three downward-pointing antennas and two upward-looking antennas of the RASTA radar, using a modified version of the Protat and Zawadzki (1999) variational 3D wind retrieval technique. For each 5 km horizontal x 120 m vertical grid sampled below the aircraft by the cloud radar three non-colinear Doppler measurements (or two above the aircraft) are matched spatially to retrieve the two horizontal wind components (only one above the aircraft) and the sum (V_T+w), where V_T is the terminal fall speed and w the vertical wind component. Usually these two components are then separated in a second step using the so-called DOP-Z-H technique described and validated in Protat and Williams (2011). The third step of the 3D wind retrieval then consists in adding the air mass continuity equation as an additional constraint and using the three wind components and V_T retrieved at steps 1 and 2 as the first guess. This last step ensures that all the constraints are well satisfied by the 3D wind and V_T. An illustration of this process is given in Fig. 4 for a straight-flight pattern from MT-2010 within a trailing stratiform region.

However, in order to utilize the closure analysis of METHOD2, only the values near flight altitude are required. Therefore in that case, step 2 described above is modified. The flight altitude (V_T+w) is obtained by interpolating linearly the values retrieved at step 1 above and below the aircraft (second panel from top in Fig. 4), and then w measured in-situ by the inertial navigation system is subtracted to that interpolated (V_T+w) to retrieve V_T. This procedure allows for more accurate retrievals of V_T, as additional errors introduced when using step 2 described above are avoided.

METHOD2 has been applied to only one flight of the MT-2010 experiment, and the results are shown for one straight flight segment in Fig. 5. The first interesting things to note on Fig. 5 are that the different simulations of Z and V_T using different sets of am and bm coefficients span a large range of possible values of Z and V_T. It is also clearly seen that radar reflectivity provides a strong constraint for am, not so strong for bm (i.e., there is a nice separation between sets of curves which correspond to different values of am, bm being shown with a color code). That result somewhat validates the METHOD1 principle, in which Z is used to retrieve am, while b is constrained by the exponent of the A(D_{max}) relationship. For sake of comparisons, three different retrievals of am and bm are compared: using Z only as a constraint (blue line), using V_T only as a constraint (green line), and METHOD2 where both Z and V_T are used as constraints.

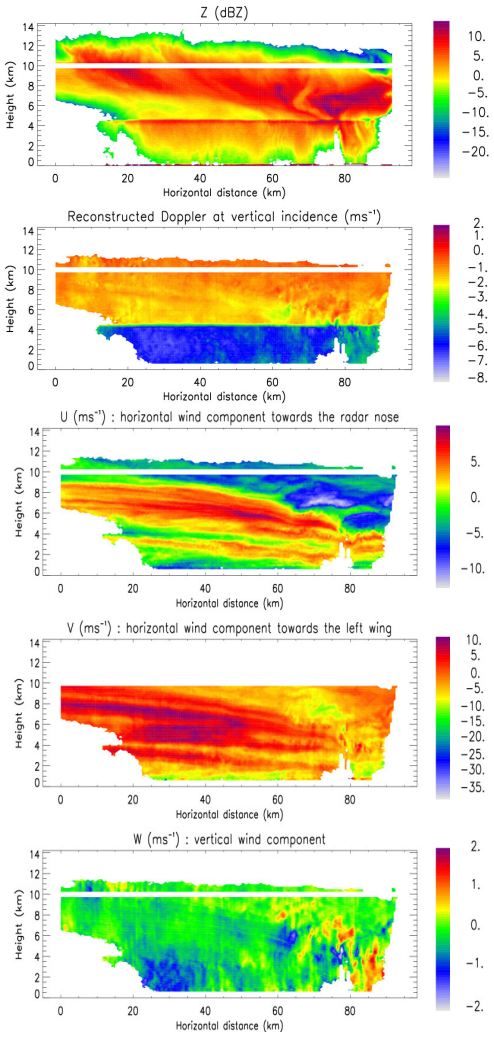

Figure 4: Illustration of the 3D wind retrieval technique. From top to bottom: radar reflectivity; (VT+w) reconstructed from the Doppler measurements; horizontal wind component towards the radar nose and towards the left wing; and the vertical wind component.

Although the three retrievals generally agree for that flight segment (it is not always the case), it is clearly observed in Fig. 5 that METHOD2 is best (as expected by construction) at fitting both Z and V_T time series observed by the RASTA radar. The retrieved am and bm values using METHOD2 scatter around the Brown and Francis (1995) am and bm parameters (dotted lines on the two bottom panels of Fig. 5), with a relatively large variability. For that single flight segment, the values of am and bm basically span the whole domain of variability set from Fig. 2. This result demonstrates that it is crucial to find ways to better constrain the m(D_{max}) relationship in active remote sensing retrievals and not use a single assumption for all clouds, and even within the same cloud. This is confirmed by the density distribution of am and bm values for a whole flight (Fig. 6). Further analysis and comparisons is required, but it seems that METHOD1 (Fig. 2) and METHOD2 (Fig. 6) seems to provide similar results regarding the span of possible am and bm coefficients in West-African stratiform precipitation.

5 CONCLUSION

The combination of airborne cloud radar data and in-situ particle size and bulk microphysics measurements is an unique way to learn more about the statistical relationship between mass, projected area, and maximum dimension of ice crystals. Our next step is to gather more data in a variety of large-scale environments in order to better understand the variability of these relationships and derive a more robust characterization of these relationships in order to estimate uncertainties in current active remote sensing retrievals of cloud microphysical properties and improve these techniques. The immediate next steps of this work will be to compare statistically the two approaches developed and check whether they can provide a consistent picture.

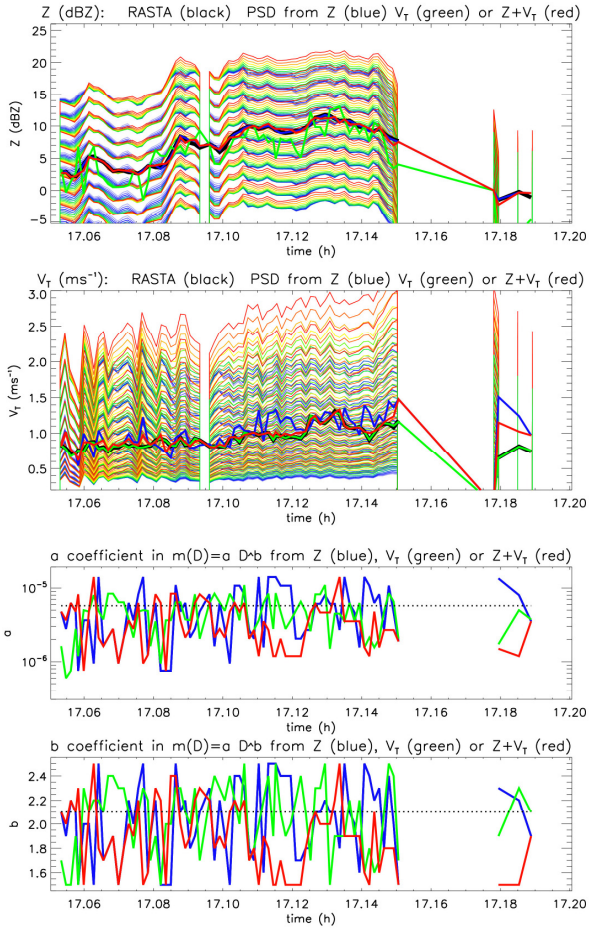

Figure 5: From top to bottom, times series of: radar reflectivity, terminal fall velocity, am, and bm. The array of curves shows the span of possible solutions when using the range of am and bm defined in Fig. 2. The black line is the RASTA radar measurement. The blue, green, and red lines are when Z, V_T, or Z and V_T are used as constraints to retrieve am and bm. The BF95 am and bm are shown as dotted lines in the two bottom panels.

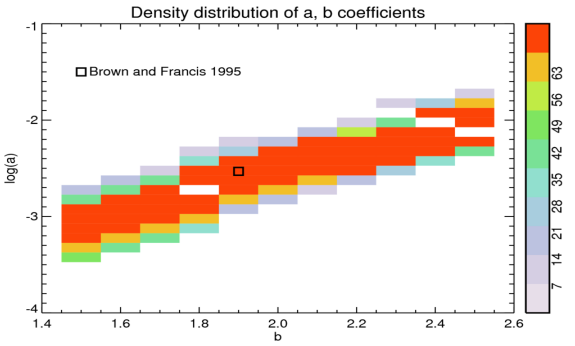

Figure 6: Density distribution of bm as a function of am for a whole stratiform precipitation flight of MT-2010.

REFERENCES

Brown, P. R. A., and P. N. Francis, 1995: Improved measurements of the ice water content in cirrus using a total-water probe. *J. Atmos. Oceanic Technol.,* **12,** 410–414.

Delanoë, J., and co-authors, 2007: The characterization of ice cloud properties from Doppler radar measurements. *J. Appl. Meteor.,* **46**, 1682–1698.

Fontaine, E., and co-authors, 2013: Constraining mass-diameter relations from hydrometeor images and cloud radar reflectivities in tropical and oceanic convection. In preparation.

Heymsfield, A. J., and C. D. Westbrook, 2010: Advances in the Estimation of Ice Particle Fall Speeds Using Laboratory and Field Measurements. *J. Atmos> Sci.*, **67**, 2469–2482.

Heymsfield, A. J., C. Schmitt, A. Bansemer, and C. H. Twohy, 2010: Improved Representation of Ice Particle Masses Based on Observations in Natural Clouds. *J. Atmos. Sci.*, **67**, 3303–3318.

Protat, A., and C. Williams, 2011: The accuracy of radar estimates of terminal fall speed from vertically-pointing Doppler cloud radar measurements. *J. Appl. Meteor. Clim,* 50, 2120-2138, doi: 10.1175/JAMC-D-10-05031.1.

Protat, A., G. McFarquhar, J. Um, and J. Delanoë, 2011: Obtaining best estimates for the microphysical and radiative properties of tropical ice clouds from TWP-ICE in-situ microphysical observations. *J. Appl. Meteor. Clim.*, **50 (4)**, 895-915.

Protat, A., and co-authors, 2009: Assessment of CloudSat reflectivity measurements and ice cloud properties using ground-based and airborne cloud radar observations. *J. Atmos. Oceanic Technol.*, **26 (9)**, 1717-1741.

Protat, A., and I. Zawadzki, 1999: A variational method for real-time retrieval of three-dimensional wind field from multiple-doppler bistatic radar network data. *J. Atmos. Oceanic Technol.*, 16 (4), 432-449.